Science of the Total Environment 878 (2023) 163016

Contents lists available at ScienceDirect

Science of the Total Environment

journal homepage: www.elsevier.com/locate/scitotenv

# Impact of flow regulation on stream morphology and habitat quality distribution

Jenna Duffin [a], Elowyn M. Yager [a], John M. Buffington [b], Rohan Benjankar [c], Carter Borden [a,d], Daniele Tonina [a,*]

[a] Center for Ecohydraulics Research, University of Idaho, Boise, USA
[b] US Forest Service, Rocky Mountain Research Station, Boise, ID, USA
[c] Southern Illinois University Edwardsville, Edwardsville, IL, USA
[d] Centered Consulting International, LLC, Boise, ID, USA

## HIGHLIGHTS

- Regulated flows reduce amplitude and frequency of pools and bars.
- Regulated flows impact fish habitat by altering stream morphology.
- Hydrologic restoration can improve subdued topography in regulated rivers.

## GRAPHICAL ABSTRACT

60 years of regulated flows formed a simpler and smother topography than that resulting from unregulated flows (left panels). The unregulated flows formed more complexy topography, with a 33 % increase in pool frequency, 92 % total pool volume and 43 % total bar volume compared to that of regulated flows. The combined effect of morphological changes and hydrology resulted in different spatial distributions of habitat suitability (CSI) and overall lower habitat quality (HHS).

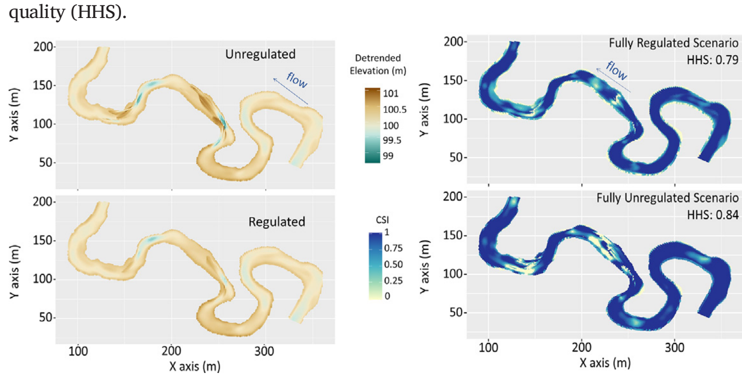


## ARTICLE INFO

Editor: Sergi Sabater

*Keywords:*
Sediment transport
Regulated and unregulated flows
Riverine habitat
Salmonids

## ABSTRACT

The importance of interactions among stream hydrology, morphology, and biology is well recognized in studies of stream ecosystems. However, when quantifying the impacts of altered flow on aquatic habitat, results are often based either on combined changes in topography and flow, or with altered flow over static topography. Here, we study the potential beneficial effects of restoring unregulated flows on salmonid habitat and separate the relative influences of changes in flow vs. topography. We hypothesize that flow restoration will increase topographic complexity and that the coevolution of topography with altered streamflow will produce stronger changes in habitat than predicted for static topography. We address this hypothesis by quantifying spawning and juvenile rearing habitat distributions for Chinook salmon (*Oncorhynchus tshawytscha*) from a set of quasi-three-dimensional hydromorphodynamic models for two morphologically distinct reaches along the Lemhi River, Idaho (USA): an engineered, straightened, plane-bed reach, and a less-altered, meandering, pool-riffle reach. Sediment transport was modeled with hydrographs predicted for actual interannual variability of flow and for a synthetic annual flow representing the ensemble actual hydrographs for 60 years of regulated and unregulated flows. The actual and synthetic hydrographs predicted from the model produced similar morphologic results, which implies that interannual flow variation and hydrograph order did not have a strong effect on the modeled topography. Unregulated hydrographs enhanced the geometry and frequency of pools in the meandering reach compared to regulated flows. These morphological changes did not increase habitat quality predicted

* Corresponding author.
*E-mail address:* dtonina@uidaho.edu (D. Tonina).

http://dx.doi.org/10.1016/j.scitotenv.2023.163016
Received 6 December 2022; Received in revised form 28 February 2023; Accepted 19 March 2023
Available online 23 March 2023

from suitability indices, but the large growth of pools likely improved winter refugia for juvenile salmon. In the straight reach, both regulated and unregulated scenarios resulted in a plane-bed morphology, suggesting that flow restoration in highly altered reaches is not sufficient to improve ecological function.

## 1. Introduction

Human alterations of rivers have led to worldwide concern over degradation of aquatic ecosystems and the need for stream habitat enhancement (Geist and Hawkins, 2016). To aid in restoration design and site selection, quantifying aquatic habitat and the processes of habitat loss are critical to identifying potential impacts of restoration (Beechie et al., 2008; Roni et al., 2008). The natural flow regime, which represents the quantity, timing, and variability of flow, is a primary driver for physical habitat and ecological integrity in river ecosystems (Poff et al., 1997; Richter et al., 2003) and interruptions to functional flows can reduce physical and biological diversity (Hayes et al., 2018; Wohl, 2012). Flow regulation has been linked to an overall reduction in geomorphic complexity, decreases in channel area, and losses in river longitudinal and lateral connectivity (Brandt, 2000; Graf, 2006; Williams and Wolman, 1984). Reductions in flow have also decreased the number and area of high bars, increased channel stability and river straightening, and reduced competent flows for sediment transport (Church, 1995; Grant et al., 2003; Ligon et al., 1995). All of these geomorphic effects, coupled with reduced flows, have generated a decrease in fish abundance and habitat in human-altered rivers (Bunn and Arthington, 2002; García et al., 2011; Poff and Zimmerman, 2010). Therefore, in rivers with modified hydrographs, it is important to consider how channel morphology may adjust as the flow regime changes (Yarnell et al., 2015) because physical habitat, specifically depth, velocity, and bedforms, results from the interaction between hydrologic regimes, channel morphology, and hydraulics (Brierley and Fryirs, 2000; Pasternack and Brown, 2013).

Although the importance of river morphology to physical habitat, and specifically to salmon habitat, is known (Cram et al., 2017; Geist and Dauble, 1998; Hanrahan, 2007; Montgomery et al., 1999), habitat is often modeled in terms of altered flow over static topography (e.g., Bovee et al., 1998) or based on combined changes in topography and flow (e.g., García et al., 2011). As topographic data and morphodynamic modeling become more accessible, some studies have considered dynamic topography. Using repeat topographic surveys, Wheaton et al. (2009) monitored a restoration project after a spring flood event and found that areas of scour were associated with reduction in salmon spawning habitat and areas of deposition led to improved spawning habitat. Another study used a coupled hydraulic and sediment transport model to identify the unregulated flow conditions needed to scour fines and expose coarse spawning substrate for white sturgeon (McDonald et al., 2010). Despite these advances, results tend to focus on short-term changes (1-10 years), warranting additional studies that consider the long-term morphodynamics of a system and its influence on habitat (Kail et al., 2015), as well as separating the impacts of altered flow regime from morphological changes on habitat under future flow scenarios.

To study the effects of flow changes on topography, the hydrology in numerical modeling and laboratory flume studies has been characterized by either actual hydrographs depicting the full variability of a system or with representative repeated hydrographs to simplify calculations and to better constrain the impacts of specific hydrograph characteristics. Flume experiments have shown that increases in discharge variability, represented by multiple high flow hydrographs, increase channel width (Vargas-Luna et al., 2019), whereas variation in the order of hydrographs affects bedform morphology (Nelson et al., 2011). Duration and frequency of individual hydrographs can affect channel slope and topographic variability (Plumb et al., 2020), but conversely the shape and duration of repeated hydrographs may have little effect on channel characteristics such as slope and sediment transport rates (Nelson and Morgan, 2018; Wong and Parker, 2006). The effects of hydrograph characteristics vary in the literature and there is limited research directly comparing the morphologic impact of variable vs. cycled simplified hydrographs (Huthoff et al., 2010). Thus, work is needed to quantify differences between actual and synthetic hydrograph inputs on modeled geomorphic response and consequent aquatic habitat.

Altering flows in rivers also may have different effects depending on the existing morphology, which mediates the effectiveness of flow restoration strategies (Meitzen et al., 2013), highlighting the fact that the current morphologic condition of rivers must be considered when studying the potential effects of deregulated flows. For example, aquatic habitat in river reaches with more physical diversity, such as those with pools and riffles, is generally more resilient to changes in flow than habitat in plane-bed rivers (Hauer et al., 2012). Similarly, restoration of natural flow regimes may not be successful in cases where humans have confined channels through levees and other structures that alter the range of fluvial processes and channel morphologies compared to historic conditions (Wohl et al., 2015; Yarnell et al., 2015). Consequently, when assessing the potential effects of changing flow regimes, it is necessary to consider the range of existing morphologic conditions and how they may mediate the potential resulting topography because the interaction between morphology and flow regime impacts the temporal and spatial variability of local hydraulics with important ecological implications (Gostner et al., 2013, 2017, 2021).

In this study, to address the potential changes in physical habitat from alterations in both flow and morphology, we developed a set of morphodynamic models for two morphologically distinct reaches: (1) a straight, highly-altered reach and (2) a meandering, more-natural reach on the Lemhi River (central Idaho, USA). The Lemhi River is an ideal study area because flows have been regulated for decades by irrigation diversion throughout the system and the river supports anadromous fish species listed under the U.S. Endangered Species Act (NMFS, 2019). Our goal was to model the morphodynamic effects of regulated vs. unregulated flows on salmonid habitat and to separately understand the effects of altered hydraulics and morphology. We hypothesized that the current regulated riverbed morphology is subdued and that unregulated flows will increase topographic complexity and, through this altered morphology, improve the availability of suitable spawning habitat and juvenile overwintering habitat. We also tested the hypothesis that interannual hydrologic variability would affect the modeled morphodynamics; this was examined by comparing the results of predicted actual hydrographs (representing interannual variability) to cycled synthetic hydrographs (no interannual variability) for both regulated and unregulated flows. Improved understanding of geomorphic and hydraulic changes from flow deregulation, and the impact of these changes on salmonid habitat, could be used to help meet restoration goals through water management and dynamic channel response, as opposed to constructed habitat improvements, such as placement of wood debris or channel realignment.

## 2. Methods

### 2.1. Study area

The Lemhi River is a 100 km-long gravel-bedded river draining a 3300 km$^2$ basin before flowing into the Salmon River in Idaho, USA (Fig. 1). Like many streams in the western USA, it has a history of hydrologic regulation due to irrigation diversions that affect the magnitude and timing of flows throughout the year, but primarily cause reduced spring and summer flows. The entire river and its floodplain were mapped at 1 m resolution with the airborne topobathymetric LiDAR EAARL-B system in October 2013 during low flow and clearwater conditions (Tonina et al., 2019).

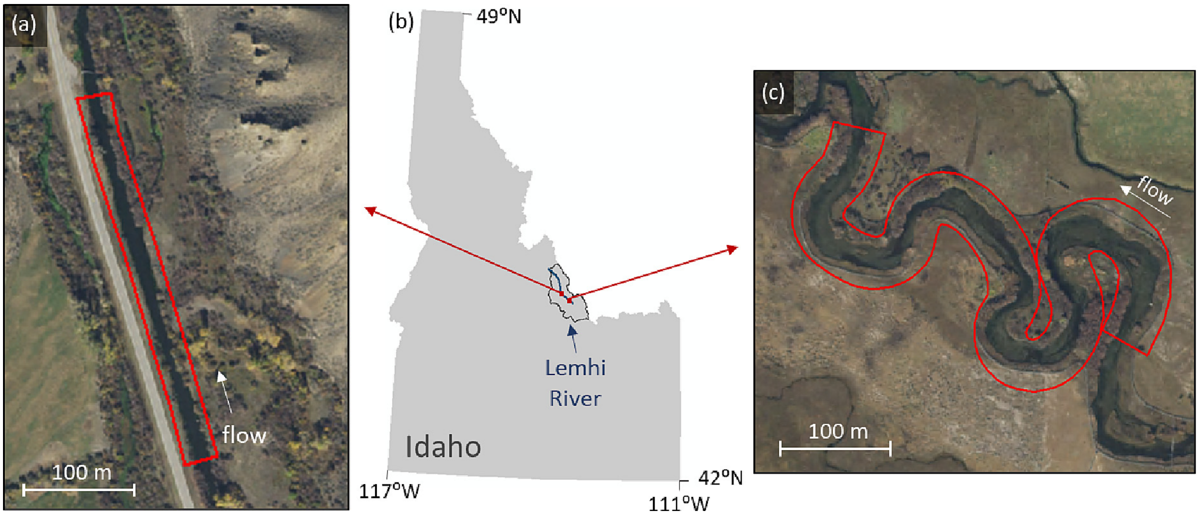


**Fig. 1.** Map of the modeling extent for the (a) straight and (c) meandering reaches and their locations within (b) the Lemhi watershed in Idaho (USA).

We selected two morphologically distinct reaches to encompass the degree of potential human alteration: an engineered straightened reach representative of the highly altered sections of river, and a less-altered, more natural and highly sinuous meandering reach (Fig. 1). The 350 m-long straight reach is channelized and flows along the highway with an average bankfull channel width of 14 m and a channel slope of 0.006 m/m. A surface median grain size ($D_{50}$) of 46 mm was measured in the reach during low flow in 2020 with (Wolman, 1954) pebble count, which was representative of the entire active area. The 650 m-long meandering reach, located ~20 km upstream of the straight reach, flows through a narrowed floodplain area confined by agricultural fields. This reach had a sinuosity of 2.8, average bankfull width of 15 m, and channel slope of 0.003 m/m. Due to limited access, a grain-size distribution was not available for this reach; instead, we used a $D_{50}$ of 36 mm, which was measured with a Wolman pebble count in 2020 in a naturally meandering reach with a similar bankfull width, depth, and slope and was located 10 km downstream of our reach with no tributaries between the two reaches. We collected grains from subaerial and subaqueous topography, including bars, riffles, and pools during low flow when most of the channel was wadable.

### 2.2. Hydraulic modeling

We developed two reach-scale morphodynamic models using the Flow and Sediment Transport with Morphological Evolution of Channels (FaSTMECH) software developed by the U.S. Geological Survey and hosted by the International River Interface Cooperative (Nelson et al., 2016; Nelson et al., 2003). FaSTMECH is a quasi-steady, quasi-3D solver, that simulates sediment transport and channel bed evolution and efficiently handles long time scales. We input the 1 m resolution LiDAR point elevations into FaSTMECH and used template mapping, a curvilinear inverse distance interpolator, to interpolate the stream and floodplain topography. We selected model grid sizes for each reach based on preliminary testing for a resolution that created the most stable model. We used a 1 m by 0.4 m (downstream by cross-stream direction) and a 1.5 m by 1 m-averaged cell size for the curvilinear grid for the straight and meandering reaches, respectively. To create a stable downstream boundary in each model, we used a 10 m grid extension and forced no recirculation at the boundary. The upstream and downstream boundary conditions were set by the flow discharge and stage.

FaSTMECH requires characterization of the lateral eddy viscosity and a roughness value quantified by a drag coefficient, which remains constant for all discharges. The lateral eddy viscosity was quantified as $0.01uh$, where $u$ and $h$ are the reach-averaged flow velocity and water depth, respectively (Tonina and Jorde, 2013). The drag coefficient was selected to minimize the mean and standard deviation of the residuals between the measured and predicted water-surface elevations and velocities. In the straight reach, 15 measurements of depth and depth-averaged velocity were collected with an ADV (acoustic Doppler velocimeter) along the channel centerline during low flow conditions (~2.3 $m^3/s$). In the meandering reach, field measurements were limited; therefore, the drag coefficient was selected by comparing FaSTMECH hydraulics with 30 depths and velocities (at 1.5 $m^3/s$) extracted along the reach centerline from a larger whole-Lemhi River hydraulic model (Tonina et al., 2020). The whole-river model was calibrated with widely spaced depth and velocity field measurements, three of which were in our meandering reach and were used to validate the selection of the drag coefficient. In the straight reach, we selected a drag coefficient of 0.01, which resulted in a mean error of 0.01 m for the water-surface elevation and a standard deviation of 0.05 m. For velocity, the mean error was 0.13 m/s or 16 % of the mean relative error (mean of the residuals normalized by the measured velocity) and a standard deviation of 0.22 m/s or 29 % of the relative error. In the meandering reach, we selected a spatially constant drag coefficient of 0.015, which resulted in a water-surface mean error of −0.02 m and a standard deviation of 0.08 m, and a velocity mean error of 0.03 m/s or 10 % of the relative error and a standard deviation of 0.10 m/s or 21 % of the relative error. These errors are similar to those reported in the literature for similar river systems (Kammel et al., 2016; Tonina and Jorde, 2013).

### 2.3. Morphodynamic modeling

To simulate bedload transport, we selected the Yalin (1963) single-grain-size equation based on $D_{50}$, similar to Nelson et al., 2015b who found that this equation produced similar bars compared to a mixed grain-size model. This allowed faster and more reliable convergence of the numerical solution than using a multi-size bedload transport equation. For each model, we allowed the flow to develop fully before calculating sediment transport by setting sediment transport to begin 60 m (about 4 bankfull channel widths) downstream of the upstream model boundary. Due to a lack of bedload transport data for the reaches, we assumed that the sediment input at the transect where sediment transport begins was equal to the calculated transport rate at that location (e.g., Nelson et al., 2015b). As the streambed evolved, the local flow depth changed, not only as a function of discharge, but also from erosion and depositional processes. These changes affect the numerical stability of the model if they occur too suddenly. Thus, we ran the models with an initial time step of 8640 s (1/10 of a day) that was adjusted with the automatic time stepping option to limit change in water depth for each cell to 2 % of the previous time step.

After preliminary model runs, we found that the shear stresses on the bed were likely overpredicted because they resulted in sediment transport at low flows when no transport had been visually observed at the field sites and they created instabilities in the models at high flows. To reduce the shear stress, we used shear stress partitioning to determine the stress acting on the particles as opposed to that borne by topographic roughness of the bed and banks (e.g., Yager et al., 2012). For a channel composed of grain and bedform roughness, the ratio of the grain shear stress ($\tau'$) to the total shear stress ($\tau_0$) can be determined from the following equation developed for dune-like bedforms (Bennett, 1995; Nelson et al., 1993; Smith and McLean, 1977)

$$\frac{\tau'}{\tau_0} = \frac{1}{1 + \frac{C_d}{2\kappa^2}\frac{\Delta}{\lambda}\left(\ln\left(\frac{0.368\Delta}{z_0}\right)\right)^2}, \quad (1)$$

where $C_d$ is the bedform drag coefficient with a value of 0.2 for separated flow, $\kappa$ is von Karman's constant with a value of 0.4, $\Delta$ is the height of the bedform, $\lambda$ is the bedform wavelength, and $z_0$ is the gain-size roughness height calculated as $0.2D_{50}$. No actual dune-like bedforms were present in these reaches, but we found that a bedform height of 0.1 m and wavelength of 0.8 m produced the minimum reduction in shear stress (~13 % reduction in the straight reach and ~17 % in the meandering reach) needed for the regulated flows (see next section) to maintain pools that were of similar depths to those initially in the reaches which, in turn, improved model stability at high flows. The partitioning likely accounted for small-scale topographic variations in the bed that were smaller than those captured by the LiDAR survey and discretized by the numerical mesh. The impact of gravitational forces due to cross-stream topographic slope, e.g., bar and pool slopes, on transverse bedload transport is parameterized in FaSTMECH with a user-defined gravitational correction based on either a pseudo-stress or a slope correction. We adopted the slope correction option and ran a set of preliminary simulations with correction values ranging between 1.2 and 2 (Nelson et al., 2015a). Results showed that increasing the slope correction value produced more subdued topographical features, e.g., less deep pools and lower bars (Nelson et al., 2015a). We selected a constant value of 1.4 because it correctly simulated bed topography, i.e., pool sizes and pool slopes, observed in the field for regulated flow conditions.

### 2.4. Hydrology

We represented the hydrology with regulated and unregulated flow scenarios from a basin-wide hydrologic model, the Lemhi River Basin Model (LRBM), which was developed to evaluate diversion operations and tributary reconnections in the Lemhi River basin. The LRBM simulates daily water allocation and in-stream discharge in the system from October 1, 2007, to September 30, 2017, by accounting for: catchment inflows; routing of water within the stream network; and diversion operation, consumption, and return flows from irrigation. The LRBM was built using the DHI MIKE BASIN software (DHI, 2003, 2006) and included lumped rainfall-runoff models (Nedbør-Afstrømnings) to predict inflow to the system, and a water allocation model to route water in the stream network and account for agricultural water use. The stream network in the LRBM was determined from the national hydrography dataset, with delineation of catchments based on a 30 m digital elevation model (DEM) (DHI, 2006). The agricultural irrigation network, represented by 322 water user nodes, was constructed from known points of diversion, places of use, aerial photography, and consultation from local water authorities and stakeholders. Historic diversion records or full water rights were used for water demand, and consumptive rates were determined by crop coefficients and reference evapotranspiration records reported by ETIdaho (Allen and Robison, 2017). The unregulated flow regime was reconstructed from the regulated flow regime and historical water use information. Further details of the LRBM can be found elsewhere (DHI, 2006).

We ran each reach-scale morphodynamic model for 60 years to ensure that the models had enough time to reach dynamic equilibrium (defined as volumes of aggradation and degradation varying around a quasi-steady mean) and to model the long-term effects of the flow scenarios. To create our 60-year hydrograph inputs for the morphodynamic models, we used a 10-year LRBM simulation and repeated this sequence of flows six times for the regulated and unregulated flow scenarios (Fig. 2). Hydrographs were available for the straight reach, but not for the meandering reach. Instead, we used the hydrograph of the reference reach used to quantify the $D_{50}$ of our meandering reach. No tributaries that would affect the magnitude of the hydrographs existed between the two meandering reaches; therefore, we used the available reference meandering reach hydrographs as a proxy for our reach even though some differences may exist from diversions. We define the hydrographs predicted from the LRBM as "actual" hydrographs to differentiate them from a set of synthetic annual hydrographs (see below). Comparison of duration curves for actual hydrographs in the straight reach showed a 45 % mean increase in flow for unregulated conditions compared to regulated flows. Unregulated flow also increased the base flow (90 % exceedance probability) by 106 %, the median flow by 22 %, the high flow (10 % exceedance probability) by 36 %, and flow variance by 30 % (Figs. S2a and b). In the meandering reach, the actual unregulated flow regime increased the mean flow by 60 %, base flow by 87 %, median flow by 22 %, high flow by 38 %, and flow variance by 24 %.

We ran each of our morphodynamic models with both actual hydrographs and a cycled, synthetic, annual hydrograph for both regulated and unregulated flows (Fig. 2). The topography resulting from the 60-year simulation of regulated flows was used as a reference for comparison with the other scenarios examined in the study. We also compared the results of the 60-year simulation of regulated flows with current topography to ensure that the numerical model properly predicts the observed streambed topography that has resulted from historic flow regulation. The actual hydrographs were used to represent interannual natural variability of flows, while the synthetic hydrographs represented the ensemble probability of flows that occurred within the 10 years of LRBM simulations and were repeated annually. We used these synthetic hydrographs to understand if the variability and sequence of annual flows affected the resulting topography. To create the synthetic annual hydrograph, we calculated the probability of all 10 years of daily flows and then subsampled probabilities, selecting a low flow at 97.5 % probability, then flows representing 5 % increments of probability from 95 % to 10 % exceedance. High flows were sampled with increasing frequency to accurately capture their occurrence down to the smallest probability of 0.027 %, which represents 0.1 day or the timestep of our model (for values see Supplementary Information). The shape of the synthetic hydrograph was based on a time-averaged (over 10 years) hydrograph for each of the actual regulated and unregulated scenarios. We shifted each of the 10 actual hydrographs in the series such that each annual peak flow occurred on the same day of the water year and then calculated the average daily flow over the 10 years. We used the shape of the averaged hydrograph for each scenario to create the synthetic hydrographs by arranging the subsampled flows into the same order of flows as the average hydrograph (see Supplementary Information). For each reach, a synthetic annual hydrograph was created for regulated and unregulated conditions and each synthetic hydrograph was repeated 60 times to create the full synthetic hydrograph time series.

### 2.5. Topographic analysis

For each reach, the models were run for 60 years of regulated and unregulated scenarios with both the actual and synthetic hydrographs for a total of four scenarios per reach. For each model scenario, we saved the stream topography at the end of each year and calculated the difference between each successive year's topographies to calculate the annual reach volumes of aggradation and degradation. We compared the final topography after 60 years among the scenarios by calculating the DEM of difference (DOD). To visualize all of the topographic data, we detrended the bed elevations by removing the reach slope from the topography and vertically translated the data by 100 m to create only positive detrended elevations.

We also extracted thalweg profiles through the final, 60-year topography of each model scenario. From these thalwegs, we identified pools by their residual depths, calculated as the difference between the deepest

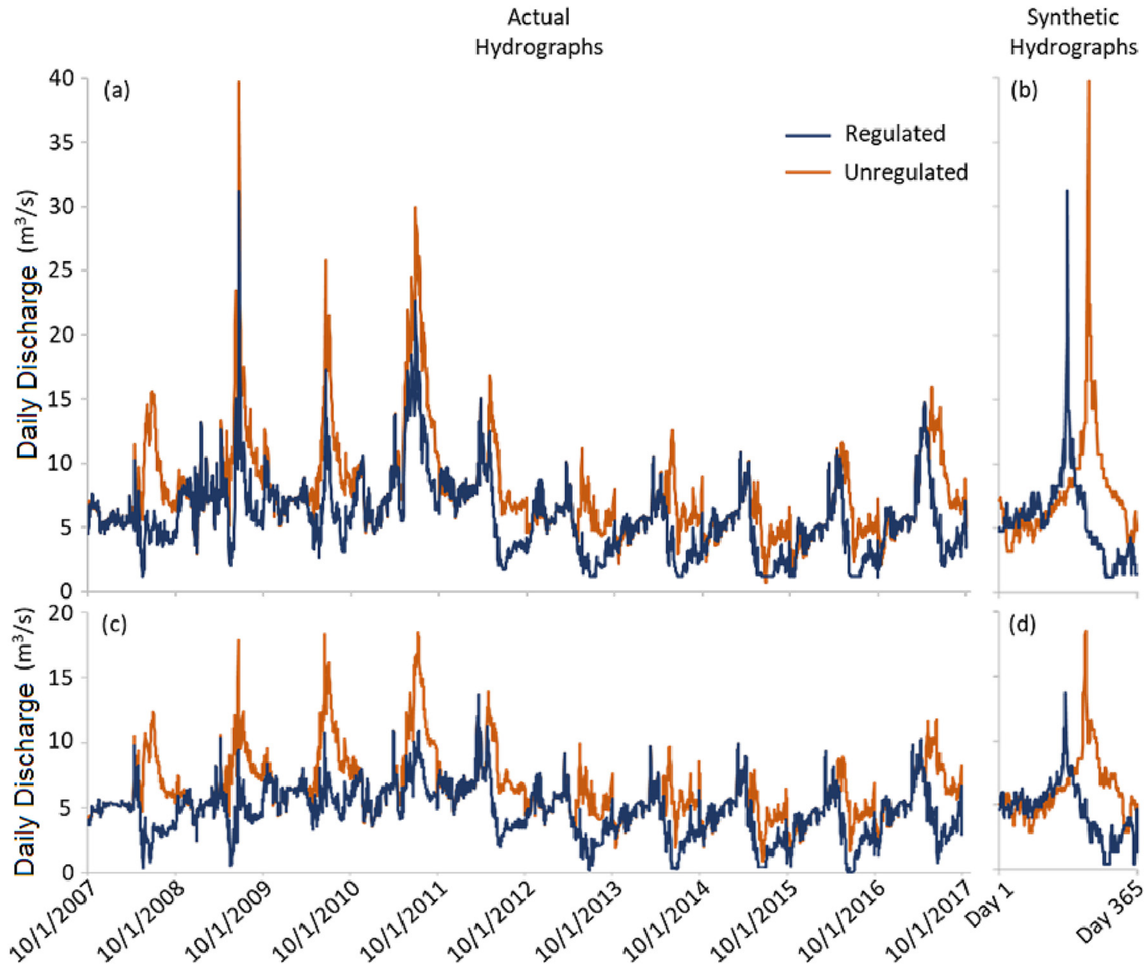


**Fig. 2.** Hydrograph scenarios used for the morphodynamic models. Hydrographs for the straight reach: (a) 10 years of actual regulated and unregulated hydrographs predicted from the LRBM (repeated six times for the model), and (b) the synthetic hydrograph for the regulated and unregulated water year (repeated 60 times for the model). Hydrographs for the meandering reach: (c) 10 years of actual regulated and unregulated hydrographs predicted from the LRBM (repeated six times for the model), and (d) the synthetic hydrograph for the regulated and unregulated water year (repeated 60 times for the model).

point in the pool and the downstream high point at the pool tail; features with residual depths larger than the threshold value of 0.4 of the reach-averaged bankfull depth (defined from the 1.5-year flow of a given scenario) were identified as pools (as defined in Duffin et al., 2021). A complimentary approach was used to identify bars from extracted longitudinal profiles of the highest point within each grid cross section after deleting points within a meter of the channel edge to reduce the effects of steep banks on residual bar heights. The highest point on each bar was compared to the downstream low point of the profile, with bars identified if they were larger than 0.4 of the reach-averaged bankfull depth.

### 2.6. Habitat analysis

In each reach, for both regulated and unregulated conditions, we quantified median flows in the fall (August and September) for both adult spawning and juvenile rearing of Chinook salmon (*Oncorhynchus tshawytscha*), as well winter flows (December and January) for juvenile rearing (Table 1). Using the hydraulic models for each reach, depths and velocities for each of these discharges were modeled on the final topographies developed from regulated and unregulated flows respectively. The fully regulated conditions represented the regulated fall or winter flows (Table 1) modeled on the final topography produced by regulated flows. Likewise, the fully unregulated conditions were the unregulated flows modeled on the final topography from unregulated conditions. To assess the relative impact of flow versus topography on habitat, the hydraulics for regulated flows were also modeled on the static, final, 60-year topography from unregulated flows and the hydraulics for unregulated flows were also modeled on the static, final, 60-year topography from regulated conditions. The habitat was assessed on the final topography produced from the actual hydrographs (further explained in the Results). For each reach and discharge, habitat quality was calculated for each model cell, CSI (cell suitability index), using suitability index curves for Chinook salmon that were empirically developed for the Upper Salmon basin (Maret et al., 2005) (see Appendix B for curves).

For each habitat discharge (Table 1), the suitability index of the *i*th cell within the model was quantified from the geometric mean of flow depth, *d*, and velocity, *v*; $\mathrm{CSI}_i = \sqrt[2]{d_i \cdot v_i}$. We then grouped the CSI values into categories: 0 to 0.2 — no habitat, 0.2 to 0.4 — low quality, 0.4 to 0.6 — moderate quality, 0.6 to 0.8 — high quality, and 0.8 to 1 — excellent quality habitat. For each reach and scenario, we calculated the total available habitat in

**Table 1**
Habitat discharges based on median flows for each season for regulated and unregulated scenarios in each reach.

| Reach | Season | Regulated discharge scenario ($m^3/s$) | Unregulated discharge scenario ($m^3/s$) |
|---|---|---|---|
| Straight | Fall | 3.5 | 7 |
| Straight | Winter | 5.5 | 5.5 |
| Meandering | Fall | 3.5 | 6 |
| Meandering | Winter | 5 | 5 |

terms of the weighted usable area (WUA) and hydraulic habitat suitability (HHS)

$$\mathrm{WUA} = \sum_{i=1}^{n} A_i \cdot \mathrm{CSI}_i, \tag{2}$$

$$\mathrm{HHS} = \frac{\mathrm{WUA}}{\sum_{i=1}^{n} A_i}, \tag{3}$$

where $A_i$ is the area of each model cell. Note that CSI, WUA and HHS are all functions of discharge.

Overwintering juvenile salmonids may have different habitat needs from other seasons because low water temperatures and ice formation may limit foraging behavior and growth (Brown et al., 2011; Huusko et al., 2007). When water temperatures decline below 3–6 °C, fish shift behavior from rearing and foraging to conserving energy, resting, finding velocity refugia, and hiding from predators and anchor ice. During this period, their metabolism is quite slow, such that they may not fully digest captured prey. Consequently, habitat suitability curves used to quantify juvenile habitat, which only consider foraging and rearing, do not fully account for juvenile winter habitat needs, such as access to low velocities and deep water refugia (Favrot et al., 2018; Huusko et al., 2007). Therefore, we also assessed winter juvenile habitat in terms of specific habitat features, such as pool depths and volumes.

## 3. Results

### 3.1. Model validation: topographic change

All model scenarios for the straight and meandering reaches attained dynamic equilibrium by the third decade for the unregulated flows, and within one decade for the regulated flows, shown by net zero sediment volume change each year or the balance between aggradation and degradation (Fig. 3). After dynamic equilibrium was attained, only small topographic changes occurred for regulated conditions. We repeated in-channel topographical surveys for the straight reach and for a meandering reach similar to that studied here but with easy access between 2011 and 2013. Comparison among years showed no in-channel elevation changes >10 cm. This confirms that the lack of annual topographic change predicted for the regulated scenarios reasonably represents current river conditions, where the $D_{50}$ is rarely mobile, and the current channel morphology is mostly stationary due to a long history of flow regulation. No unregulated field sites were available to test topographic results of the unregulated scenarios.

### 3.2. Sediment transport

The morphodynamic models only predicted substantial movement of the $D_{50}$, in more than just a few cells of the model, at the highest flows present in each reach: flows above ~23 $m^3$/s and 17 $m^3$/s for the straight and meandering reaches, respectively. These flows have recurrence probabilities of 0.94 % and 0.10 % for unregulated and regulated conditions, respectively, in the straight reach and 0.21 % and 0 % for the meandering reach. Before the models reached dynamic equilibrium, there was sediment transport at lower discharges, but after dynamic equilibrium was met only the high flows resulted in substantial sediment transport. Cumulative curves of annual aggradation and degradation increased smoothly for the synthetic hydrographs and in a stepped manner for the actual hydrographs in both reaches (Fig. 3). The latter resulted from the fact that sediment-mobilizing flows occurred during three consecutive years each decade for the actual hydrographs, whereas sediment-mobilizing flows occurred every year (albeit for a shorter duration) for the synthetic hydrographs, producing a relatively smooth increase in cumulative annual aggradation and

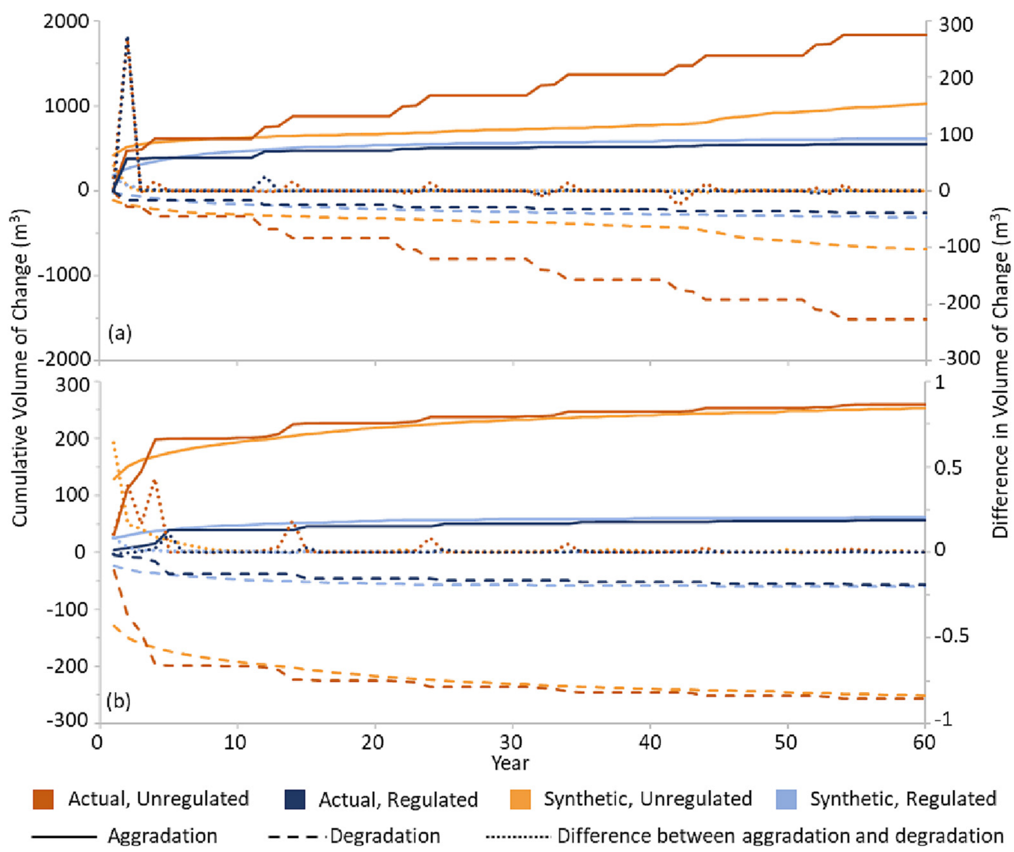


**Fig. 3.** Annual total aggradation and degradation over time for the (a) straight plane-bed reach and (b) meandering pool-riffle reach. Each hydrograph scenario is represented by a different color, cumulative aggradation over time is shown by the solid lines, cumulative degradation is shown by the dashed lines, and the annual difference between the aggradation and degradation is shown by the dotted lines.

degradation. In both reaches, unregulated flow produced substantially more cumulative aggradation/degradation than regulated flows (Fig. 3), but reach-specific differences in behavior were also predicted.

In the straight reach, the final aggradation and degradation volumes were similar for the regulated flow scenarios (Fig. 3a). In contrast, larger volumes of aggradation and degradation occurred for actual flows than synthetic ones during unregulated conditions in the straight reach (Fig. 3a). In the unregulated actual scenario, after the first decade of model adjustment, the first high flow of each decade washed out a series of subdued bedforms (proto-bars and pools) and topographic undulations, and then the second and third high flows rebuilt these subdued bedforms, but the topography at the beginning and end of a given decade was similar. This pattern of washing out and rebuilding subdued bedforms in the straight reach did not occur with the unregulated synthetic hydrographs, which resulted in less aggradation and degradation over time.

In the meandering reach, the actual and synthetic hydrographs produced similar final volumes of aggradation/degradation for a given flow scenario, with unregulated flow exhibiting larger cumulative volumes (Fig. 3b). Fully formed pool-riffle topography in the meandering reach resulted in a more stable bed (less volumetric change over time) and no appreciable difference in the effects of actual vs. synthetic hydrographs compared to the repeated washing out and rebuilding of proto-bedforms in the straight, plane-bed reach during unregulated flow with actual hydrographs.

### *3.3. Actual versus synthetic hydrographs: morphologic differences*

Here, we compare the effects of actual versus synthetic hydrographs on the final channel topography for each flow scenario (regulated or unregulated). The effects of the flow scenarios on channel morphology are examined in the next section.

In the straight reach, actual and synthetic hydrographs produced a similar, final, plane-bed topography (Figs. 4g and h) with comparable thalweg profiles (Fig. 5a). Specifically, 82 % and 97 % of the model cells exhibited less than $\pm 0.1$ m difference in elevation between topographies developed from actual vs. synthetic hydrographs for the unregulated and regulated flows respectively. In the unregulated scenario, the larger differences in topography between synthetic and actual hydrographs (Fig. 4g) resulted from location differences in the pattern of the final topography rather than development of different overall morphologic patterns. This is highlighted by the thalweg differences between the actual and synthetic hydrographs for the unregulated scenario, specifically at 200 m where a subdued pool-like bedform created by the actual hydrographs is not present in the synthetic hydrograph profile but is instead shifted downstream to 240 m (Fig. 5a).

Similarly, differences in elevation for the final topography of the meandering reach were small for actual vs. synthetic hydrographs (Figs. 6g and h) and the thalweg profiles were comparable for a given flow scenario (regulated or unregulated, Fig. 5b). Most model cells exhibited $\pm \sim 0.1$ m difference in elevation for actual vs. synthetic hydrographs, with aggradation and degradation localized to areas of forced pools and bars. For example, in the unregulated scenario, only 0.2 % of the model cells exhibited large differences in elevation ($\pm \sim 0.5$ to 1 m) between topographies produced from the actual and synthetic hydrographs, with these differences caused by a shift in the location of the pools or bars (Figs. 6a, d, and g).

The above results indicate that the interannual variability and sequence of hydrographs did not greatly affect the final topography in either of the study reaches and that both synthetic and actual hydrographs can be used to represent the hydrology when modeling morphology for a given flow scenario (regulated or unregulated). Consequently, to simplify the remaining analyses, results will be based on the topography produced by actual hydrographs from this point forward, recognizing that the findings would be similar for synthetic hydrographs.

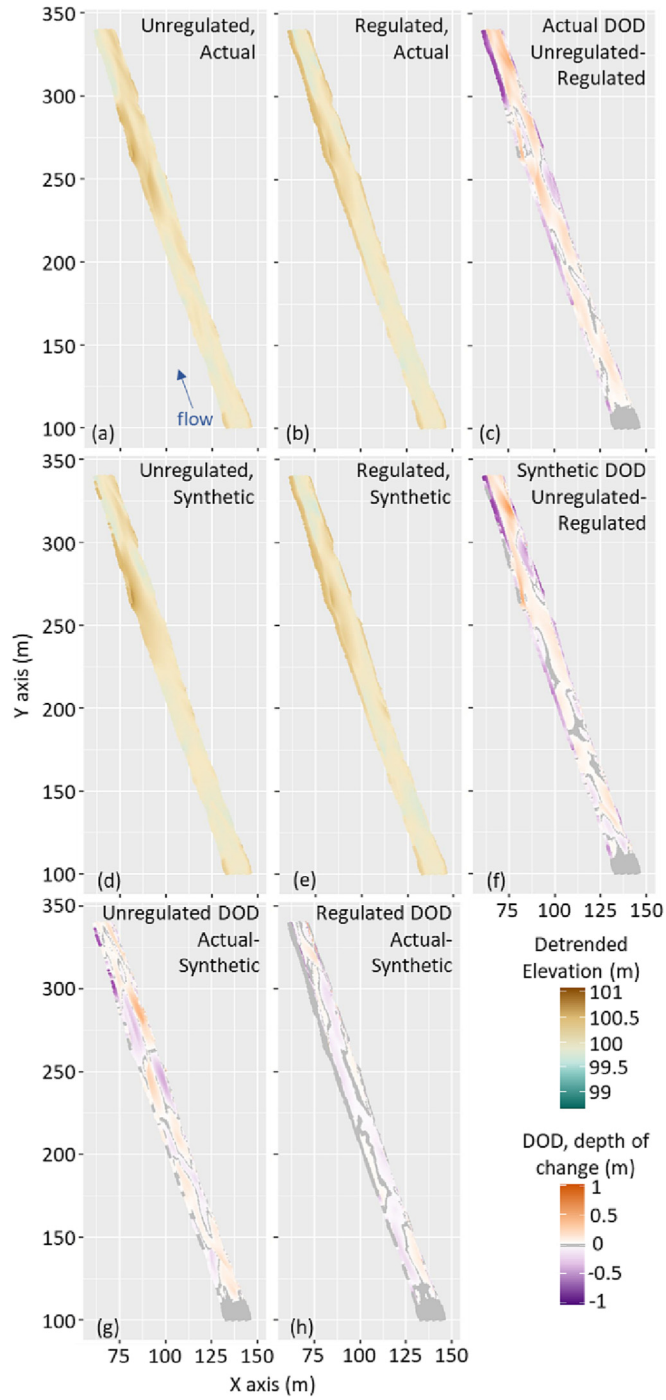


**Fig. 4.** The final, 60-year, modeled straight reach topography for each hydrograph scenario: (a) unregulated, actual hydrographs, (b) regulated, actual hydrographs, (d) unregulated, synthetic hydrographs, and (e) regulated, synthetic hydrographs. Digital elevation models (DEMs) of difference (DODs) between the different final topographies are shown for (c) unregulated minus regulated actual scenarios, (f) unregulated minus regulated synthetic hydrographs, (g) actual minus synthetic unregulated scenarios and (h) actual minus synthetic regulated scenarios. Note that the detrended elevations and DOD maps are shown on the same scale as the meandering reach in Fig. 6, which has a wider range of elevations and depths of change.

### *3.4. Regulated versus unregulated flows: morphologic differences*

The final topography of the straight reach exhibited a plane-bed morphology with no significant pools or bars for both regulated and unregulated flows. For all scenarios in the straight reach, the final detrended

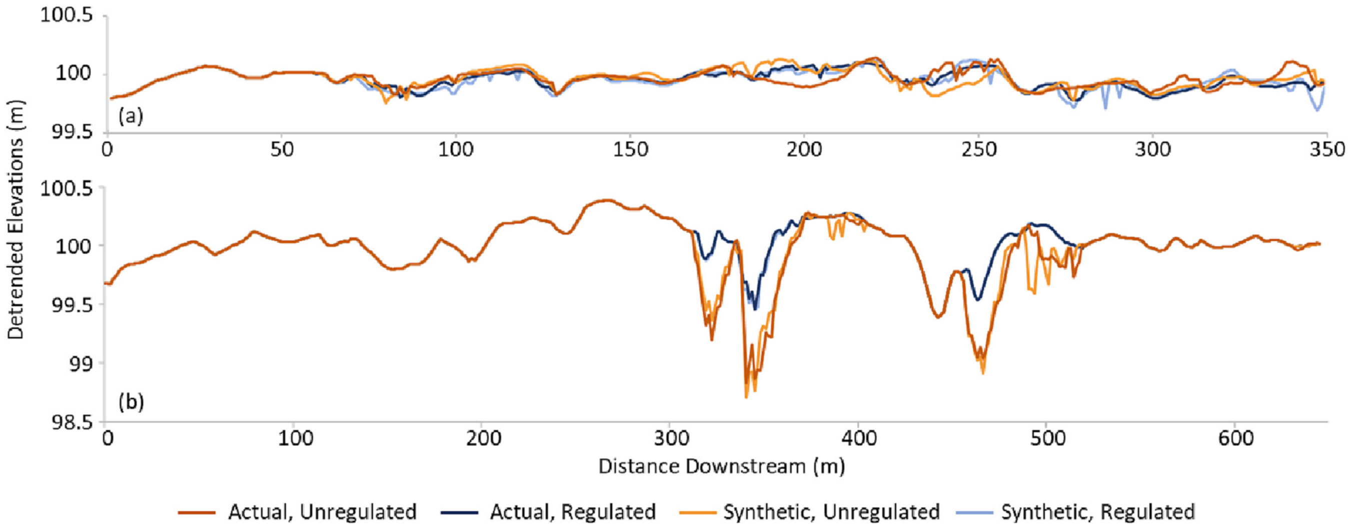


**Fig. 5.** Detrended thalweg profiles for the final topography in the (a) straight plane-bed reach and (b) meandering pool-riffle reach. The profiles for each hydrograph scenario are shown in different colors; some lines are not visible where they overlap other lines.

thalwegs show 0.35 m of vertical range with a standard deviation of 0.07 m (Fig. 5a). Comparison of the final topographies for regulated vs. unregulated flows showed mostly small differences in elevation for actual and synthetic hydrographs (Figs. 4c and f, respectively); 66 % of model cells had differences in elevation less than ±0.1 m, with some larger differences (never larger than 0.6 m) due to either slight shifting in the topographic patterns or to locations at the downstream end of the reach, which may be affected by the downstream model boundary.

In the meandering reach, regulated flows formed more subdued pool-riffle morphology compared to unregulated flows. Topographic variability in the detrended thalweg profile increased from a vertical range of 1.00 to 1.55 m between regulated and unregulated flows and the standard deviation increased from 0.18 to 0.27 m (Fig. 5b). The unregulated flows scoured pools deeper than the regulated scenario and the scoured sediment built larger downstream bars, resulting in 8.6 % of model cells having differences in elevation greater than ±0.1 m between topographies generated from regulated and unregulated flows for both actual and synthetic hydrographs (Figs. 6c and f). Pool and bar geometry (area, volume, and maximum depth/height) all increased between regulated and unregulated flow (Fig. 7), and a new pool formed during unregulated flow, resulting in a 33 % increase in pool frequency. Total pool volume increased by 92 % and total bar volume increased by 43 % between regulated and unregulated flows.

For both the regulated and unregulated conditions, the meandering reach showed more topographic variability and complexity than the straight reach, which is highlighted by the final thalweg profiles (Fig. 5)

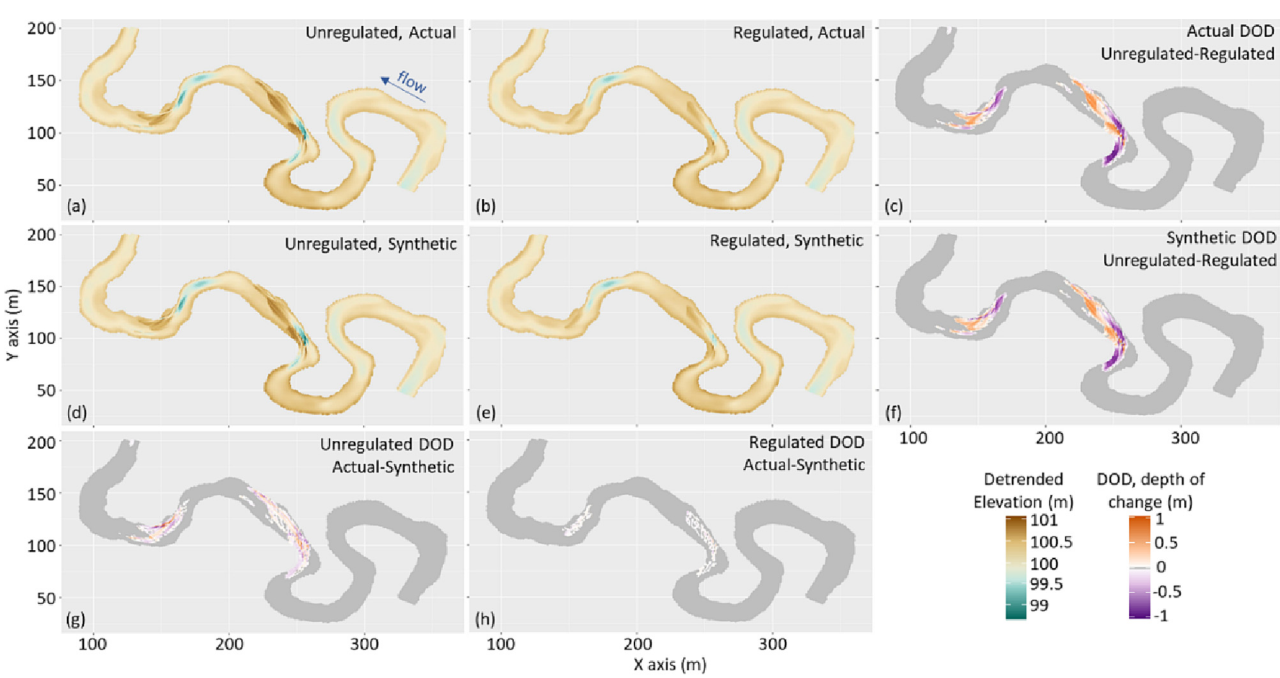


**Fig. 6.** The final, 60-year, modeled meandering reach topography for each hydrograph scenario: (a) unregulated, actual hydrographs, (b) regulated, actual hydrographs, (d) unregulated, synthetic hydrographs, and (e) regulated synthetic hydrographs. Digital elevation models (DEMs) of difference (DoDs) between the different final topographies are shown for (c) unregulated minus the regulated actual scenarios, (f) unregulated minus the regulated synthetic hydrographs, (g) actual minus the synthetic unregulated scenarios and (h) actual minus the synthetic regulated scenarios.

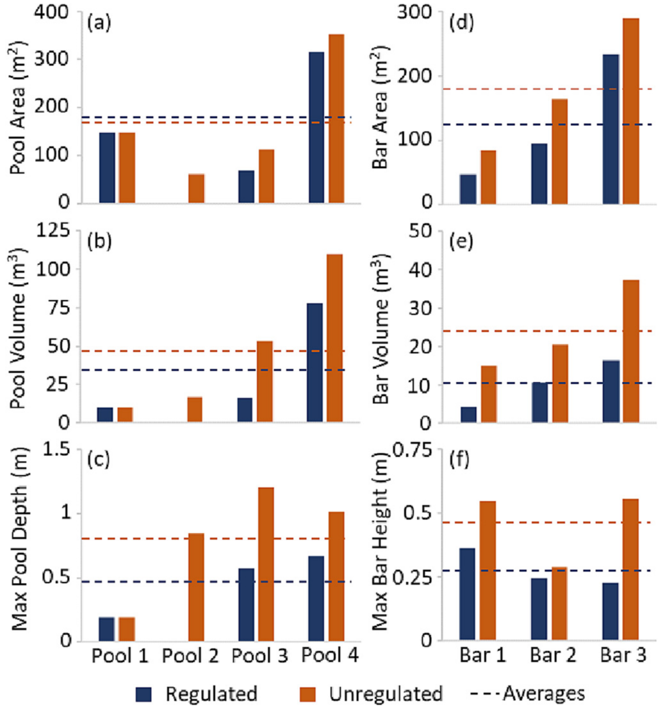


**Fig. 7.** Distributions of pool and bar geometry in the meandering reach for regulated and unregulated flows: (a) pool area, (b) pool volume, (c) maximum pool depth, (d) bar area, (e) bar volume, and (f) maximum bar height. Color indicates flow type (regulated vs. unregulated) and dashed lines are average values of each distribution.

and by comparing the elevation ranges for the final topographies, where the straight and meandering reaches had total detrended elevation ranges of 1.05 and 2.32 m, respectively (Figs. 4 and 6).

In both reaches, differences in regulated vs. unregulated flow conditions produced stronger changes in sediment transport and final reach topography than choice of actual vs. synthetic hydrographs (Figs. 3–6). Furthermore, unregulated flow resulted in greater topographic variability in the meandering reach by scouring deeper pools and depositing higher bars than the topography formed by regulated flow. In contrast, the plane-bed morphology of the straight reach was less responsive to differences in flow condition (regulated vs. unregulated).

### 3.5. Regulated versus unregulated flows: habitat differences

The fully regulated condition (i.e., regulated flows on topography developed from those flows) in the straight reach produced more suitable habitat for fall spawning of Chinook salmon (HHS = 0.41) and a greater abundance of high-quality habitat than the fully unregulated condition (HHS = 0.15) (Figs. 8a and S3a–b). Regulated conditions produced lower fall flows that improved the spawning habitat quality and availability compared to higher flow velocities associated with unregulated flow. Furthermore, flow condition (regulated vs. unregulated) and the associated channel hydraulics were a stronger control on habitat than the effect of flow on the final topography; HHS values of 0.15 occurred for unregulated flow in the straight reach regardless of whether the final topography was produced from regulated or unregulated flow, and nearly identical HHS values of 0.41 and 0.42 resulted from regulated flow over the respective straight-reach topographies. In addition, the straight reach had little to no available winter habitat for juvenile Chinook salmon (HHS = 0.01) for all flow and topography conditions (Figs. 8c and S4a–b). The juvenile rearing habitat in this reach was greatly limited by high velocities in both the fall and winter, which were almost entirely outside the suitability range for juvenile Chinook salmon for both the regulated and unregulated flows regardless of the topography (Fig. S5b–d).

In the meandering reach, fall spawning habitat quality was adequate in all tested flow and topography conditions, but was higher for fully unregulated conditions (HHS = 0.84) than fully regulated (HHS = 0.79) (Figs. 8b and S3d–e). This increase in modeled habitat suitability was not due to differences in final topographies (i.e., whether they were formed by regulated or unregulated flow), but directly to differences in the hydraulics of those flows over the topography. High unregulated flows in the fall increased habitat on both topographies (both HHS = 0.84), whereas the relatively smaller regulated flows resulted in slightly lower HHS values of 0.79 for both topographies. Although the HHS values for the regulated and unregulated flows on the topography developed from unregulated flows were similar, the unregulated topography resulted in a 2–5 % increase (depending

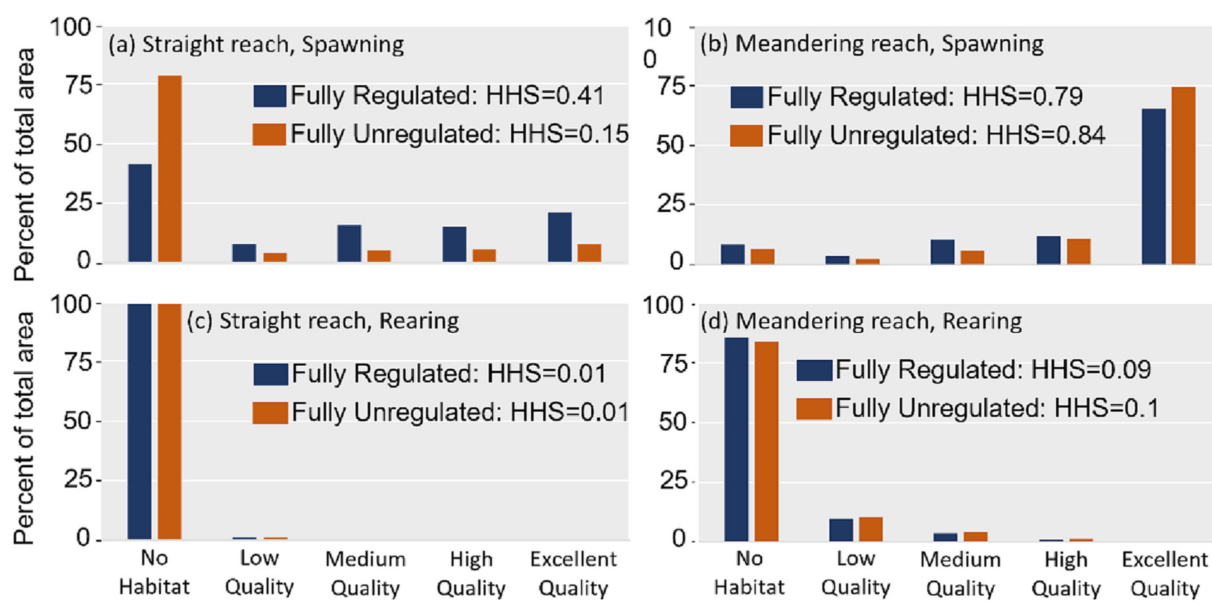


**Fig. 8.** Habitat quality distributions for fall spawning Chinook salmon (top panels) in (a) the straight and (b) meandering reaches and for winter rearing (bottom panels) in (c) the straight and (d) meandering reaches for regulated topography and regulated flow (i.e., fully regulated conditions; blue histograms) and for unregulated topography and unregulated flow (i.e., fully unregulated conditions; dark orange histograms). (For interpretation of the references to color in this figure legend, the reader is referred to the web version of this article.)

on flow condition) in excellent quality spawning habitat compared to the topography developed from regulated flows (Fig. 8b).

Availability of winter habitat for rearing of juvenile Chinook salmon remained similar between the fully regulated (HHS = 0.09) and fully unregulated (HHS = 0.10) conditions in the meandering reach (Figs. 8d and S4d–e). The regulated and unregulated winter flows were the same (Table 1); therefore, these small differences were entirely attributable to changes in the topography developed from each flow type. The high and excellent-quality winter juvenile habitat was mainly on the margins of the channel, where the velocities were low. In most of the meandering reach, velocities were too high in both the fall and winter to produce suitable juvenile rearing habitat for both the regulated and unregulated flows regardless of the topography (Figs. S5f and h). However, slightly more juvenile rearing habitat was available in the meandering reach than the straight one (cf. Figs. 8c and d; cf. Figs. S5b and d to f and h).

## 4. Discussion

Our hypothesis of subdued topography for regulated flows was borne out for the meandering reach, but not the plane-bed reach. However, the increased topographic variability produced by unregulated flows in the meandering reach did not substantially increase habitat availability and quality, at least in terms of HHS values; nevertheless, increased pool depths may provide important overwintering refugia for juvenile salmonids that is not detected by the HHS analysis. Surprisingly, the largest increases in spawning habitat availability and diversity were driven by lower velocities for the regulated flow in the plane-bed reach despite no substantial changes in topography, underscoring the relative roles of flow vs. topography and the fact that results can vary with channel type (plane-bed vs. pool-riffle).

### *4.1. Actual versus synthetic hydrographs*

Our results show that actual hydrographs (representative of the natural interannual variability of flows) and synthetic hydrographs (a single, cycled, representative hydrograph) both produced similar morphologic patterns in each of our study reaches. Flume studies assessing the impact of the shape and duration of cycled hydrographs have found varying results; in some cases, those factors had little influence on bedform and channel characteristics (Nelson and Morgan, 2018; Wong and Parker, 2006), whereas other studies have found hydrograph shape and duration had an impact on bedload flux (Redolfi et al., 2018) and channel morphology (Waters and Curran, 2015; Zhang et al., 2020). Another study addressed the effect of flow order and found that changing the location of a uniform high-flow period within low flows resulted in similar bedform geometry (Nelson et al., 2011). A morphodynamic modeling study looking at the effects of cycled hydrographs found that a single, repeated, representative hydrograph produced aggradation and degradation outside of the range produced by hydrographs representing variability in discharge (Huthoff et al., 2010), but suggested the representative hydrograph may have been oversimplified by not including the full range of flows. Phillips et al. (2018) showed that bedload flux resulting from a variety of hydrograph shapes scaled with transport capacity, suggesting that maintaining transport capacity between hydrograph comparisons may provide more similar morphologic results; however, many of these studies did not hold transport capacity constant between their compared hydrographs, which may explain the variation in results. Therefore, representative designed hydrographs should preserve some physical properties of the hydrology, such as the peak discharge, volume of flows, and hydrograph shape that accurately represents the full probability of flows (Serinaldi and Grimaldi, 2011). The synthetic hydrographs presented in this paper accurately represented the full probability of flows present in the actual hydrographs and reproduced the hydrograph shape, therefore producing similar final bed elevations and topographic features compared to those resulting from temporally variable hydrographs. Fully and accurately representing the high flows in this system was important because the $D_{50}$ only moved at the highest flows, which is similar to what has been observed in other similar systems (Andrews, 1994; Maturana et al., 2013; McKean and Tonina, 2013).

### *4.2. Regulated versus unregulated flows: morphologic differences*

The meandering reach model showed that regulated flows resulted in more subdued topography, whereas the unregulated flows produced larger pool and bar geometry (i.e., greater area, depth/height, and volume), as well as increased pool frequency than the regulated scenarios. The current channel topography has adjusted to years of flow regulation with reduced magnitudes and durations of high flows that are needed to maintain pools and bars (e.g., Caamaño et al., 2009; MacWilliams et al., 2006; Sawyer et al., 2010). The current absence of high flows in the Lemhi River combined with our model results suggest that the river previously may have had more topographic variability, with deeper pools and more pronounced bars. Increasing the occurrence of high flows in regulated rivers will not only improve topographic variability, but also has important ecological effects. The unregulated high flows help to create an active river bed, which can remove fines and clean spawning gravels (Milhous, 1998; Reiser et al., 1989) and can break up armor layers (Parker and Klingeman, 1982; Ryan et al., 2005; Vericat et al., 2006; Yager et al., 2015). We did not measure the subsurface grain size distribution and therefore could not determine the extent of bed armoring. However, the median surface grain size only moved during high flows in our models, which implies a relatively stable surface layer particularly during the regulated flows. Given that the surface layer usually protects the finer subsurface layer from erosion, we would expect more fines to potentially accumulate in the bed during regulated than unregulated flows (Dikinya et al., 2008; Schälchli, 1992).

Topographic differences between the various flow scenarios were more pronounced in the meandering reach, where pools and bars were already present, than in the straight reach. The occurrence of topographic steering (Whiting and Dietrich, 1991), flow convergence (MacWilliams et al., 2006; Thompson and Wohl, 2009), or a combination of these effects (Brown and Pasternack, 2014) over the initial pool-riffle topography helped to maintain and further develop this topography in the meandering reach. In contrast, such processes do not emerge in the straight, planar reach. Consequently, restoration of flows alone may not be sufficient to regenerate or improve channel morphology in highly altered reaches (Wohl et al., 2015) such as the straight reach, where the existing variability in topography and lack of channel curvature is not sufficient to develop pools and bars in our simulations.

Results from modeling studies like this have limitations based on how the model is conceptualized and implemented. For example, we used a sediment transport model based on a single grain size, ignoring the potential effects of grain size interactions, such as particle hiding and size-selective transport, that could result in errors in bedload predictions (Durafour et al., 2014). Multi-size sediment transport may allow for the evolution of armor layers and formation of textural patches that may impact bar, riffle, and pool morphologies. However, the morphological effects of using a full grain-size distribution compared to a single grain size when modeling channel evolution may be minimal as shown by numerical modeling (Nelson et al., 2015b). Similarly, the adoption of a spatially constant drag coefficient may lead to the formation of bars with shorter wavelengths and higher amplitudes than those with a spatially variable roughness (Nelson et al., 2015b). Conversely, accounting for a full grain-size distribution with smaller sediment may reduce the modeled depths and volumes of pools as a result of low-flow sand deposition in the pools (Thompson et al., 1996). Including patch-based (e.g., riffle versus pool) grain-size information is also important in accurately predicting sediment transport, but may not be as important as the spatial variability in flow and shear stress (Monsalve et al., 2016), which was included in these models. Nor does our approach consider history-dependent critical shear stress values, which can impact bedload transport based on the previous flow magnitudes (Masteller et al., 2019; Reid et al., 1985; Turowski et al., 2011). Without large flow events regularly mobilizing the bed, channel stabilization can occur as the critical shear stress increases each year due to low and moderate flows (An et al., 2021; Masteller et al., 2019). The dependence of critical shear stress on flow magnitude and flood sequencing could affect the modeled morphological differences we saw between the synthetic and actual hydrographs. The interannual variability in flows in the actual hydrographs would affect the critical shear stress and the order of the flows could be more important than we showed, whereas the synthetic hydrographs, with annual high flows, would be less affected.

### 4.3. Regulated versus unregulated flows: habitat differences

Both regulated and unregulated flows produced moderate to high amounts of spawning habitat in both reaches, except for the fully unregulated scenario in the straight reach (HHS = 0.15). Furthermore, differences in topography developed from regulated vs. unregulated flows had very little effect on the availability of spawning habitat. The increased fall flows under the unregulated scenario affected the spawning suitability differently in each reach; spawning habitat was substantially reduced in the straight reach and slightly increased in the meandering reach.

Previous studies have shown that juvenile habitat, specifically overwintering habitat, is a limiting factor in the Lemhi River (Carmichael et al., 2020; Copeland et al., 2014). Contrary to our expectations that unregulated flow would increase habitat abundance and quality due to less subdued morphology compared to regulated conditions, we only predict a 1 % increase in habitat suitability for winter juvenile rearing between fully regulated and fully unregulated scenarios in the meandering reach. For all flow scenarios, the depth-averaged velocities were higher than suitable for juvenile Chinook rearing (Fig. S5), therefore no substantial increase in juvenile rearing habitat was predicted based on suitability curves. Nevertheless, changes in predicted pool geometry and frequency may be important. The 33 % increase in pool frequency, 36 % expansion in pool area, 92 % growth in pool volume, and 54 % increase in maximum residual pool depth between the regulated and unregulated scenarios in the meandering reach (Fig. 7) does not affect juvenile habitat suitability (Fig. 8d), but may have local benefits not detected by the suitability curves. In particular, diverse habitat with deep pools act as refugia from high velocities, create stable conditions during discharge changes (Moir et al., 2006), and increase the probability of overwintering survival for juvenile salmonids (Brown et al., 2011). Although the modeled HHS values for juvenile rearing habitat are unresponsive to regulated vs. unregulated conditions in the meandering reach, juvenile fish can use the lower velocities at the bottom of these deeper pools (Favrot et al., 2018). A study of microhabitat use in a similar stream found that Chinook parr disproportionally occupied the deepest water available during fall and winter rearing, specifically deep water areas >1.15 m (Favrot et al., 2018). During regulated fall flow (3.5 $m^3/s$) in the meandering reach, the area of the channel with depths >1.15 m increased from 1.7 $m^2$ to 104.2 $m^2$ (6029 % increase) between topographies developed from regulated vs. unregulated flow, and from 30.9 $m^2$ to 145 $m^2$ (372% increase) for the unregulated fall flow (6 $m^3/s$) on those topographies, highlighting the relative importance of the change in topography compared to the change in flows. For regulated and unregulated winter flows (5 $m^3/s$) in the meandering reach, the streambed area with depths >1.15 m increased from 13.0 $m^2$ to 130.5 $m^2$ (902% increase), resulting in a substantial increase in deep-water juvenile refugia for topography developed from unregulated flows.

### 4.4. Management implications

Our results show that unregulated flows could create more complex habitat through scouring of larger pools and increased pool frequency in the meandering reach. Instream restoration goals often include adding stream complexity by manually creating deep pool habitat and bars, and in regulated rivers, reintroduction of the highest flows may be an effective way to complete widespread restoration of subdued topography with minimal instream disturbance (Groll, 2017). We found that only the highest flows present in our reaches mobilized the $D_{50}$ and resulted in meaningful morphologic changes. In the meandering reach, for the unregulated scenario, our models demonstrated that the pools developed quickly, much of the scour occurred during the first high flow, and the pools almost reached their maximum depths after three high flow years. Each of these high flows (larger than 17 $m^3/s$) lasted approximately one day each year. However, actual timescales for morphological change in natural rivers may differ from our modeled results due to factors not accounted for in our analysis, such as bed armoring, sediment supply effects, size-selective transport, and meander migration. Changes in riparian vegetation due to climate change and land use may also impact meander migration, which we did not model. Although caveats exist, the results showing rapid development of deep, large pools are promising for water management.

Large, extreme, disturbance events have the potential to produce large shifts in habitat (Reich and Lake, 2015). Consequently, avoiding diversion during high-water years may be enough to substantially improve juvenile habitat quality. Fulltime unregulated flows may not be necessary or beneficial for improving habitat; Carmichael et al. (2020) modeled bioenergetics for juvenile salmonids over multiple reaches along the Lemhi River and found that regulated flows produced more favorable conditions for juvenile growth than unregulated flows. Although Carmichael et al. (2020) did not account for potential changes in channel topography, they highlight the importance of slow water and lateral habitat refugia during unregulated flow conditions. We also show that the impact of flow restoration on instream morphology is not enough to reduce high velocities during fall and winter flows, which highlights the importance of lateral habitat reconnection and the potential addition of large wood to aid in velocity reduction if diversions were removed for extend periods of time.

Although we focused on the potential effects of unregulated flows on two reaches along the Lemhi River, restoration of natural flows at basin scales may have larger benefits. Our straight-reach model showed that channelized, highly-altered reaches may not improve with flow restoration (Groll, 2017; Wohl et al., 2015), but less altered reaches may have potential for morphologic improvement. Specifically, in the meandering reach, pool and bar volumes increased greatly from unregulated flows. To identify how much of the Lemhi River could possibly result in improved habitat from restoration of unregulated flows, we calculated the portion of the river having similar topographic variability to that of the meandering reach. A previous study on the Lemhi River found that small-scale wavelet power quantifies topographic variability of the thalweg and was representative of pool-riffle topography (Duffin et al., 2021). Based on the observed, small-scale, wavelet power of the meandering reach, we found that 93 % of the Lemhi River has similar or higher topographic variability. This portion of the river represents areas with existing pools, which are subdued from decades of flow regulation, while the remaining 7 % of the river is composed of highly-altered reaches without existing pool-riffle topography. Although 93 % of the river has similar (or better) topographic variability to the meandering reach, only 65 % of the Lemhi River is meandering (sinuosity >1.2) and it is unknown if the sinuous reaches have a stronger response potential than less sinuous locations. The potential to improve juvenile overwintering habitat through basin-wide flow restoration along this river by increasing channel complexity and increasing pool geometry and frequency is much larger than the potential effects of local, instream, habitat improvements (e.g., woody-debris placement or channel realignment) because of the considerable area that basin-wide flow restoration could impact. Increases in deep pool habitat could also improve the resiliency of the river to potential climate change stresses due to reduced flows (Walters et al., 2013) by providing consistent hydraulic and thermal refugia (Justice et al., 2017).

## 5. Conclusion

Hydromorphodynamic models can help to assess the effects of water management strategies on both stream hydraulics and morphology. Our analysis revealed the differences in reach topography, hydraulics, and habitat between regulated and unregulated flows applied over a 60-year period for an engineered, straightened, plane-bed reach and a more natural meandering reach. We tested a series of predicted hydrographs that represent the actual interannual variability of flows vs. a synthetic, cycled, annual hydrograph that is a composite of the actual flows. The actual and synthetic hydrographs after 60 years of simulation resulted in similar final modeled topographies for both reaches. The $D_{50}$ was mobile only at the highest flows present in these reaches, with both the actual and synthetic hydrographs having the same probability for high-flow occurrence. We find that the sequence and interannual variability of flows was not as important as the occurrence of sediment-mobilizing high flows. Consequently, both hydrograph types (actual and synthetic) produced similar topographic results in a given reach.

For the straight reach, we found that the topography remained plane-bed between the regulated and unregulated flow scenarios, and spawning habitat quality for Chinook salmon was negatively affected by relatively higher unregulated discharges. Juvenile rearing habitat in the fall and winter was essentially non-existent for both the regulated and unregulated scenarios due to velocities that exceeded suitability.

In the meandering reach, unregulated flows resulted in more spatially variable topography than occurred for regulated flows, with a notable increase in pool depth, volume, and frequency. The change in topography between the regulated and unregulated flow scenarios had a negligible effect on Chinook salmon spawning habitat, which was high for both flow scenarios. Nevertheless, the increased pool geometry and frequency resulting from unregulated flows may benefit juveniles by providing greater fall and winter refugia.

Hydrologic restoration can improve subdued topography in currently regulated rivers like those examined in our study. Because high flows are capable of moving the $D_{50}$ at our sites, increasing the frequency and magnitude of high flows may have the potential to scour subdued pools and build larger bars. Restoring unregulated high flows may improve in-channel morphology where bedforms are present (e.g., meandering pool-riffle channels), but is likely to have limited effect in reaches lacking bedforms or sinuosity, such as the engineered straightened reach. Instead, those sites may need more intervention than hydrologic restoration alone. A complex response between hydrology, topography and habitat exists; and the use of morphodynamic models, and the analysis of both hydrologic and morphologic changes together, can be a powerful tool to help water managers make informed decisions that will have the greatest benefit to the ecological function of rivers.

## CRediT authorship contribution statement

JD ran the 2D modeling, CB ran the hydrological model, RB provided large scale 2D modeling, and DT envisioned the research and administered the funding. JD wrote the original version of the manuscript. All authors contributed to the interpretation of the results and in editing the manuscript.

## Data availability

Data are available from Tonina et al. (2022) at the repository site HydroShare (http://www.hydroshare.org/resource/73fac6d628bc43e48a1801bad8f93f45).

## Declaration of competing interest

Authors declare no competing interests.

## Acknowledgments

This research was partially supported by the Idaho Office of Species Conservation (grant number LEM023 16), by the Bonneville Power Administration (Project # 2010-072-0), and by the U.S. Forest Service (grant number 16-CR-11221634-049). We thank Biomark Inc. for logistical support and for facilitating access to data, land, and streams. Data are available from HydroShare (Tonina et al., 2022)

## Appendix A. Supplementary data

Supplementary data to this article can be found online at https://doi.org/10.1016/j.scitotenv.2023.163016.

## References

Allen, R.G., Robison, C.W., 2017. Evapotranspiration and consumptive irrigation water requirements for Idaho: supplement updating the time series through December 2016, Research Technical Completion Report. Kimberly Research and Extension Center, University of Idaho, Moscow, ID Retrieved from http://www.kimberly.uidaho.edu/ETIdaho/.

An, C., Hassan, M.A., Ferrer-Boix, C., Fu, X., 2021. Effect of stress history on sediment transport and channel adjustment in graded gravel-bed rivers. Earth Surf. Dyn. 9 (2), 333–350. https://doi.org/10.5194/ESURF-9-333-2021.

Andrews, E.D., 1994. Marginal bed load transport in a gravel bed stream, Sagehen Creek, California. Water Resour. Res. 30 (7), 2241–2250. https://doi.org/10.1029/94WR00553.

Beechie, T., Pess, G., Roni, P., Giannico, G., 2008. Setting river restoration priorities: a review of approaches and a general protocol for identifying and prioritizing actions. N. Am. J. Fish Manag. 28 (3), 891–905. https://doi.org/10.1577/m06-174.1.

Bennett, J.P., 1995. Algorithm for resistance to flow and transport in sand-bed channels. J. Hydraul. Eng. 121 (8), 578–590. https://doi.org/10.1061/(asce)0733-9429(1995)121:8(578).

Bovee, K.D., Lamb, B.L., Bartholow, J.M., Stalnaker, C.B., Taylor, J., Henriksen, J., 1998. Stream habitat analysis using the instream flow incremental methodology. U.S. Geol. Surv., Bio. Resour. Div. Inform. Tech. Rep. USGS/BRD-1998-0004, 131.

Brandt, S.A., 2000. Classification of geomorphological effects downstream of dams. Catena 40 (4), 375–401. https://doi.org/10.1016/S0341-8162(00)00093-X.

Brierley, G.J., Fryirs, K., 2000. River styles, a geomorphic approach to catchment characterization: implications for river rehabilitation in Bega catchment, New South Wales, Australia. Environ. Manag. 25 (6), 661–679. https://doi.org/10.1007/s002670010052.

Brown, R.A., Pasternack, G.B., 2014. Hydrologic and topographic variability modulate channel change in mountain rivers. J. Hydrol. 510, 551–564.

Brown, R.S., Hubert, W.A., Daly, S.F., 2011. A primer on winter, ice, and fish: what fisheries biologists should know about winter ice processes and stream-dwelling fish. Fisheries 36 (1), 8–26.

Bunn, S.E., Arthington, A.H., 2002. Basic principles and ecological consequences of altered flow regimes for aquatic biodiversity. Environ. Manag. 30 (4), 492–507.

Caamaño, D., Goodwin, P., Buffington, J.M., Liou, J.C., Daley-Laursen, S., 2009. Unifying criterion for the velocity reversal hypothesis in gravel-bed rivers. J. Hydraul. Eng. 135 (1), 66–70. https://doi.org/10.1061/(ASCE)0733-9429(2009)135:1(66).

Carmichael, R.A., Tonina, D., Keeley, E.R., Benjankar, R.M., See, K.E., 2020. Some like it slow: a bioenergetic evaluation of habitat quality for juvenile Chinook salmon in the Lemhi River, Idaho. Can. J. Fish. Aquat. Sci. 77 (7), 1221–1232. https://doi.org/10.1139/cjfas-2019-0136.

Church, M., 1995. Geomorphic response to river flow regulation: case studies and time-scales. Regul. Rivers: Res. Manag. 11 (1), 3–22. https://doi.org/10.1002/rrr.3450110103.

Copeland, T., Venditti, D.A., Barnett, B.R., 2014. The importance of juvenile migration tactics to adult recruitment in stream-type Chinook salmon populations. Trans. Am. Fish. Soc. 143 (6), 1460–1475. https://doi.org/10.1080/00028487.2014.949011.

Cram, J.M., Torgersen, C.E., Klett, R.S., Pess, G.R., May, D., Pearsons, T.N., Dittman, A.H., 2017. Spatial variability of Chinook salmon spawning distribution and habitat preferences. Trans. Am. Fish. Soc. 146 (2), 206–221. https://doi.org/10.1080/00028487.2016.1254112.

DHI, 2003. Evaluation of diversion operation plans to meet negotiated flow targets for salmon and steelhead in the Lemhi River basin using the MIKE BASIN model. DHI, Inc. Report prepared for U.S. Bureau of Reclamation and Idaho Department of Water Resources. Boise, ID. 41 pp. Retrieved from https://www.google.com/url?client=internal-element-cse&cx=013944898621778347075:fimgx16c16i&q=https://idwr.idaho.gov/wp-content/uploads/sites/2/iwrb/2003/200304-MIKE-Basin-Model-Lemhi-River-Mainstream-Report.pdf&sa=U&ved=2ahUKEwiOwObxk_9AhU4iO4BHZQ2AW0QFnoECAIQAg&usg=AOvVaw0xMtWaqag9nkek0pfG-mY.

DHI, 2006. The Lemhi River MIKE BASIN model: a tool for evaluating stream flows, diversion operations and surface water – ground water relationships in the Lemhi River. DHI, Inc. Report prepared for U.S. Bureau of Reclamation and Idaho Governor's Office of Species Conservation through Idaho Department of Water Resources. Boise, ID 102 pp. Retrieved from chrome-extension://efaidnbmnnnibpcajpcglclefindmkaj/https://idwr.idaho.gov/wp-content/uploads/sites/2/iwrb/2006/200609-MIKE-Basin-Model-Lemhi-River-Tributaries-Report.pdf.

Dikinya, O., Hinz, C., Aylmore, G., 2008. Decrease in hydraulic conductivity and particle release associated with self-filtration in saturated soil columns. Geoderma 146, 192–200.

Duffin, J., Carmichael, R.A., Yager, E.M., Benjankar, R., Tonina, D., 2021. Detecting multi-scale riverine topographic variability and its influence on Chinook salmon habitat selection. Earth Surf. Process. Landf. 46, 1026–1040. https://doi.org/10.1002/esp.5077.

Durafour, M., Jarno, A., Le Bot, S., Lafite, R., Marin, F., 2014. Bedload transport for heterogeneous sediments. Environ. Fluid Mech. 15 (4), 731–751. https://doi.org/10.1007/S10652-014-9380-1.

Favrot, S.D., Jonasson, B.C., Peterson, J.T., 2018. Fall and winter microhabitat use and suitability for spring Chinook salmon parr in a U.S. Pacific Northwest River. Trans. Am. Fish. Soc. 147 (1), 151–170. https://doi.org/10.1002/tafs.10011.

García, A., Jorde, K., Habit, E., Caamaño, D., Parra, O., 2011. Downstream environmental effects of dam operations: changes in habitat quality for native fish species. River Res. Appl. 27 (3), 312–327.

Geist, D.R., Dauble, D.D., 1998. Redd site selection and spawning habitat use by fall Chinook salmon: the importance of geomorphic features in large rivers. Environ. Manag. 22 (5), 655–669.

Geist, J., Hawkins, S.J., 2016. Habitat recovery and restoration in aquatic ecosystems: current progress and future challenges. Aquat. Conserv.: Mar. Freshw. Ecosyst. 26, 942–962. https://doi.org/10.1002/aqc.2702.

Gostner, W., Alp, M., Schleiss, A.J., Robinson, C.T., 2013. The hydro-morphological index of diversity: a tool for describing habitat heterogeneity in river engineering projects. Hydrobiologia 712 (1), 43–60. https://doi.org/10.1007/s10750-012-1288-5.

Gostner, W., Paternolli, M., Schleiss, A.J., Scheidegger, C., Werth, S., 2017. Gravel bar inundation frequency: an important parameter for understanding riparian corridor dynamics. Aquat. Sci. 79 (4), 825–839. https://doi.org/10.1007/s00027-017-0535-2.

Gostner, W., Annable, W.K., Schleiss, A.J., Paternolli, M., 2021. A case-study evaluating river rehabilitation alternatives and habitat heterogeneity using the hydromorphological index of diversity. J. Ecohydraul. 6 (1), 1–16. https://doi.org/10.1080/24705357.2019.1680320.

Graf, W.L., 2006. Downstream hydrologic and geomorphic effects of large dams on American rivers. Geomorphology 79, 336–360.

Grant, G.E, Schmidt, J.C., Lewis, S.L., 2003. A geological framework for interpreting downstream effects of dams on rivers. In: O'Connor, J.E., Grant, G.E. (Eds.), A Peculiar River: Geology, Geomorphology, and Hydrology of the Deschutes River. American Geophysical Union, Water Science and Application 7, Washington, DC, pp. 203–219.

Groll, M., 2017. The passive river restoration approach as an efficient tool to improve the hydromorphological diversity of rivers – case study from two river restoration projects in the German lower mountain range. Geomorphology 293, 69–83. https://doi.org/10.1016/j.geomorph.2017.05.004.

Hanrahan, T.P., 2007. Bedform morphology of salmon spawning areas in a large gravel-bed river. Geomorphology 86, 529–536. https://doi.org/10.1016/j.geomorph.2006.09.017.

Hauer, C., Unfer, G., Holzmann, H., Schmutz, S., Habersack, H., 2012. The impact of discharge change on physical instream habitats and its response to river morphology. Clim. Chang. 116 (3), 827–850. https://doi.org/10.1007/S10584-012-0507-4.

Hayes, D.S., Brändle, J.M., Seliger, C., Zeiringer, B., Ferreira, T., Schmutz, S., 2018. Advancing towards functional environmental flows for temperate floodplain rivers. Sci. Total Environ. 633, 1089–1104. https://doi.org/10.1016/j.scitotenv.2018.03.221.

Huthoff, F., Van Vuren, S., Barneveld, H.J., Scheel, F., 2010. On the importance of discharge variability in the morphodynamic modeling of rivers. In: Dittrich, A., Koll, K., Aberle, J., Geisenhainer, P. (Eds.), River Flow 2010, Bundesanstalt für Wasserbau, pp. 985–992.

Huusko, A., Greenberg, L., Stickler, M., Linnansaari, T., Nykänen, M., Vehanen, T., et al., 2007. Life in the ice lane: the winter ecology of stream salmonids. River Res. Appl. 23 (5), 469–491. https://doi.org/10.1002/RRA.999.

Justice, C., White, S.M., McCullough, D.A., Graves, D.S., Blanchard, M.R., 2017. Can stream and riparian restoration offset climate change impacts to salmon populations? J. Environ. Manag. 188, 212–227. https://doi.org/10.1016/j.jenvman.2016.12.005.

Kail, J., Brabec, K., Poppe, M., Januschke, K., 2015. The effect of river restoration on fish, macroinvertebrates and aquatic macrophytes: A meta-analysis. Ecol. Indicators 58, 311–321. https://doi.org/10.1016/j.ecolind.2015.06.011.

Kammel, L.E., Pasternack, G.B., Massa, D.A., Bratovich, P.M., 2016. Near-census ecohydraulics bioverification of *Oncorhynchus mykiss* spawning microhabitat preferences. J. Ecohydraul. 1 (1–2), 62–78. https://doi.org/10.1080/24705357.2016.1237264.

Ligon, F.K., Dietrich, W.E., Trush, W.J., 1995. Downstream ecological effects of dams - a geomorphic perspective. Bioscience 45 (3), 183–192. https://doi.org/10.2307/1312557.

MacWilliams, M.L., Wheaton, J.M., Pasternack, G.B., Street, R.L., Kitanidis, P.K., 2006. Flow convergence routing hypothesis for pool-riffle maintenance in alluvial rivers. Water Resour. Res. 42 (W10427).

Maret, T.R., Hortness, J.E., Ott, D.S., 2005. Instream flow characterization of Upper Salmon River Basin streams, Central Idaho. U.S. Geol. Surv. Inves. Rep. 2005-5212 124 pp.

Masteller, C.C., Finnegan, N.J., Turowski, J.M., Yager, E.M., Rickenmann, D., 2019. History-dependent threshold for motion revealed by continuous bedload transport measurements in a steep mountain stream. Geophys. Res. Lett. 46 (5), 2583–2591. https://doi.org/10.1029/2018GL081325.

Maturana, O., Tonina, D., McKean, J.A., Buffington, J.M., Luce, C.H., Caamaño, D., 2013. Modeling the effects of pulsed versus chronic sand inputs on salmonid spawning habitat in a low-gradient gravel-bed river. Earth Surf. Process. Landf. 39 (7), 877–889. https://doi.org/10.1002/esp.3491.

McDonald, R.R., Nelson, J.M., Paragamian, V., Barton, G.J., 2010. Modeling the effect of flow and sediment transport on white sturgeon spawning habitat in the Kootenai River, Idaho. J. Hydraul. Eng. 136 (12), 1077–1092.

McKean, J.A., Tonina, D., 2013. Bed stability in unconfined gravel bed mountain streams: with implications for salmon spawning viability in future climates. J. Geophys. Res.: Earth Surf. 118 (3), 1227–1240. https://doi.org/10.1002/jgrf.20092.

Meitzen, K.M., Doyle, M.W., Thoms, M.C., Burns, C.E., 2013. Geomorphology within the interdisciplinary science of environmental flows. Geomorphology 200, 143–154. https://doi.org/10.1016/J.GEOMORPH.2013.03.013.

Milhous, R.T., 1998. Modelling of instream flow needs: the link between sediment and aquatic habitat. Regul. Rivers: Res. Manag. 14, 79–94. https://doi.org/10.1002/(SICI)1099-1646(199801/02)14:1.

Moir, H.J., Gibbins, C.N., Soulsby, C., Webb, J.H., 2006. Discharge and hydraulic interactions in contrasting channel morphologies and their influence on site utilization by spawning Atlantic salmon (Salmo salar). Can. J. Fish. Aquat. Sci. 63, 2567–2585. https://doi.org/10.1029/2010GL046558.

Monsalve, A., Yager, E.M., Turowski, J.M., Rickenmann, D., 2016. A probabilistic formulation of bed load transport to include spatial variability of flow and surface grain size distributions. Water Resour. Res. 52 (5), 3579–3598. https://doi.org/10.1002/2015WR017694.

Montgomery, D.R., Beamer, E.M., Pess, G.R., Quinn, T.P., 1999. Channel type and salmonid spawning distribution and abundance. Can. J. Fish. Aquat. Sci. 56 (3), 377–387.

Nelson, J.M., McLean, S.R., Wolfe, S.R., 1993. Mean flow and turbulence fields over two-dimensional bed forms. Water Resour. Res. 29 (12), 3935–3953. https://doi.org/10.1029/93WR01932.

Nelson, J.M., Bennett, J.P., Wiele, S.M., 2003. Flow and sediment-transport modeling. In: Kondolf, G.M., Piégay, H. (Eds.), Tools in Fluvial Geomorphology. John Wiley & Sons, Chichester, UK, pp. 539–576.

Nelson, J.M., Logan, B.L., Kinzel, P.J., Shimizu, Y., Giri, S., Shreve, R.L., McLean, S.R., 2011. Bedform response to flow variability. Earth Surf. Process. Landf. 36 (14), 1938–1947. https://doi.org/10.1002/ESP.2212.

Nelson, J.M., Shimizu, Y., Abe, T., Asahi, K., Gamou, M., Inoue, T., et al., 2016. The international river interface cooperative: public domain flow and morphodynamics software for education and applications. Adv. Water Resour. 93 (Part A), 62–74.

Nelson, P.A., Morgan, J.A., 2018. Flume experiments on flow and sediment supply controls on gravel bedform dynamics. Geomorphology 323, 98–105. https://doi.org/10.1016/j.geomorph.2018.09.011.

Nelson, P.A., McDonald, R.R., Nelson, J.M., Dietrich, W.E., 2015a. Coevolution of bed surface patchiness and channel morphology: 1. Mechanisms of forced patch formation. J. Geophys. Res.: Earth Surf. 120, 1687–1707. https://doi.org/10.1002/2014JF003428.

Nelson, P.A., McDonald, R.R., Nelson, J.M., Dietrich, W.E., 2015b. Coevolution of bed surface patchiness and channel morphology: 2. Numerical experiments. J. Geophys. Res. Earth Surf. 120 (9), 1708–1723. https://doi.org/10.1002/2014JF003429.

NMFS, 2019. Endangered Species Act section 7(a)(2) biological opinion and Magnuson-Stevens Fishery Conservation and Management Act essential fish habitat response, continued operation and maintenance of the Columbia River system. NMFS Consultation Number WCRO-2018-00152. 966 pp. plus appendices. Retreived from https://www.fisheries.noaa.gov/resource/document/continued-operation-and-maintenance-columbia-river-system.

Parker, G., Klingeman, P.C., 1982. On why gravel bed streams are paved. Water Resour. Res. 18 (5), 1409–1423. https://doi.org/10.1029/WR018i005p01409.

Pasternack, G.B., Brown, R.A., 2013. Ecohydraulic design of riffle-pool relief and morphological unit geometry in support of regulated gravel-bed river rehabilitation. In: Maddock, I., Harby, A., Kemp, P., Wood, P. (Eds.), Ecohydraulics: An Integrated Approach. John Wiley & Sons, Chichester, UK, pp. 337–355.

Phillips, C.B., Hill, K.M., Paola, C., Singer, M.B., Jerolmack, D.J., 2018. Effect of flood hydrograph duration, magnitude, and shape on bed load transport dynamics. Geophys. Res. Lett. 45 (16), 8264–8271. https://doi.org/10.1029/2018GL078976.

Plumb, B.D., Juez, C., Annable, W.K., McKie, C.W., Franca, M.J., 2020. The impact of hydrograph variability and frequency on sediment transport dynamics in a gravel-bed flume. Earth Surf. Process. Landf. 45 (4), 816–830. https://doi.org/10.1002/ESP.4770.

Poff, N.L., Allan, J.D., Bain, M.B., Karr, J.R., Prestegaard, K.L., Richter, B.D., et al., 1997. The natural flow regime. Bioscience 47 (11), 769–784. https://doi.org/10.2307/1313099.

Poff, L.N., Zimmerman, J.K.H., 2010. Ecological responses to altered flow regimes: a literature review to inform the science and management of environmental flows. Freshw. Biol. 55, 194–205.

Redolfi, M., Bertoldi, W., Tubino, M., Welber, M., 2018. Bed load variability and morphology of gravel bed rivers subject to unsteady flow: a laboratory investigation. Water Resour. Res. 54 (2), 842–862. https://doi.org/10.1002/2017WR021143.

Reich, P., Lake, P.S., 2015. Extreme hydrological events and the ecological restoration of flowing waters. Freshw. Biol. 60 (12), 2639–2652. https://doi.org/10.1111/fwb.12508.

Reid, I., Frostick, L.E., Layman, J.T., 1985. The incidence and nature of bedload transport during flood flows in coarse-grained alluvial channels. Earth Surf. Process. Landf. 10 (1), 33–44. https://doi.org/10.1002/ESP.3290100107.

Reiser, D.W., Ramey, M.P., Beck, S., Lambert, T.R., Geary, R.E., 1989. Flushing flow recommendations for maintenance of salmonid spawning gravels in a steep, regulated stream. Regul. Rivers: Res. Manag. 3 (1), 267–275. https://doi.org/10.1002/rrr.3450030126.

Richter, B.D., Mathews, R., Harrison, D.L., Wigington, R., 2003. Ecologically sustainable water management: managing river flows for ecological integrity. Ecol. Appl. 13 (1), 206–224. https://doi.org/10.1890/1051-0761(2003)013.

Roni, P., Hanson, K., Beechie, T., 2008. Global review of the physical and biological effectiveness of stream habitat rehabilitation techniques. N. Am. J. Fish. Manag. 28 (3), 856–890. https://doi.org/10.1577/m06-169.1.

Ryan, S.E., Porth, L.S., Troendle, C.A., 2005. Coarse sediment transport in mountain streams in Colorado and Wyoming, USA. Earth Surf. Process. Landf. 30 (3), 269–288. https://doi.org/10.1002/esp.1128.

Sawyer, A.M., Pasternack, G.B., Moir, H.J., Fulton, A.A., 2010. Riffle-pool maintenance and flow convergence routing observed on a large gravel-bed river. Geomorphology 114 (3), 143–160. https://doi.org/10.1016/J.GEOMORPH.2009.06.021.

Schälchli, U., 1992. The clogging of coarse gravel river beds by fine sediment. Hydrobiologia (1), 235–236.

Serinaldi, F., Grimaldi, S., 2011. Synthetic design hydrographs based on distribution functions with finite support. J. Hydraul. Eng. 16 (5), 434–446.

Smith, J.D., McLean, S.R., 1977. Spatially averaged flow over a wavy surface. J. Geophys. Res. 82 (12), 1735–1746. https://doi.org/10.1029/JC082i012p01735.

Thompson, D.M., Wohl, E.E., 2009. The linkage between velocity patterns and sediment entrainment in a forced-pool and riffle unit. Earth Surf. Process. Landf. 34 (2), 177–192. https://doi.org/10.1002/esp.1698.

Thompson, D.M., Wohl, E.E., Jarrett, R.D., 1996. A revised velocity-reversal and sediment-sorting model for a high-gradient, pool-riffle stream. Phys. Geogr. 17 (2), 142–156. https://doi.org/10.1080/02723646.1996.10642578.

Tonina, D., Jorde, K., 2013. Hydraulic modelling approaches for ecohydraulic studies: 3D, 2D, 1D and non-numerical models. In: Maddock, I., Harby, A., Kemp, P., Wood, P. (Eds.), Ecohydraulics: An Integrated Approach. John Wiley & Sons, Ltd, Chichester, UK, pp. 31–74 https://doi.org/10.1002/9781118526576.ch3.

Tonina, D., McKean, J.A., Benjankar, R.M., Wright, C.W.W., Goode, J.R., Chen, Q., et al., 2019. Mapping river bathymetries: evaluating topobathymetric LiDAR survey. Earth Surf. Process. Landf. 44 (2), 507–520. https://doi.org/10.1002/esp.4513.

Tonina, D., McKean, J.A., Benjankar, R.M., Yager, E., Carmichael, R.A., Chen, Q., et al., 2020. Evaluating the performance of topobathymetric LiDAR to support multi-dimensional flow modelling in a gravel-bed mountain stream. Earth Surf. Process. Landf. 45 (12), 2850–2868. https://doi.org/10.1002/esp.4934.

Tonina, D., Duffin, J., Benjankar, R.M., Yager, E.M., Buffington, J.M., Borden, C., 2022. Lemhi River effect of flow regulation on stream morphology. Retrieved fromHydroShare. http://www.hydroshare.org/resource/73fac6d628bc43e48a1801bad8f93f45.

Turowski, J.M., Badoux, A., Rickenmann, D., 2011. Start and end of bedload transport in gravel-bed streams. Geophys. Res. Lett. 38, L04401. https://doi.org/10.1029/2010GL046558.

Vargas-Luna, A., Crosato, P., Byishimo, Wim, S.J., 2019. Impact of flow variability and sediment characteristics on channel width evolution in laboratory streams. J. Hydraul. Res. 57 (1), 51–61. https://doi.org/10.1080/00221686.2018.1434836.

Vericat, D., Batalla, R.J., Garcia, C., 2006. Breakup and reestablishment of the armour layer in a large gravel-bed river below dams: the lower Ebro. Geomorphology 76 (1–2), 122–136. https://doi.org/10.1016/J.GEOMORPH.2005.10.005.

Walters, A.W., Bartz, K.K., McClure, M.M., 2013. Interactive effects of water diversion and climate change for juvanile Chinook salmon in the Lemhi River basin (USA). Conserv. Biol. 27 (6), 1179–1189.

Waters, K.A., Curran, J.C., 2015. Linking bed morphology changes of two sediment mixtures to sediment transport predictions in unsteady flows. Water Resour. Res. 51 (4), 2724–2741. https://doi.org/10.1002/2014WR016083.

Wheaton, J.M., Brasington, J., Darby, S.E., Merz, J., Pasternack, G.B., Sear, D., Vericat, D., 2009. Linking geomorphic changes to salmonid habitat at a scale relevant to fish. River Res. Appl. 26 (4), 469–486. https://doi.org/10.1002/rra.1305.

Whiting, P.J., Dietrich, W.E., 1991. Convective accelerations and boundary shear stress over a channel bar. Water Resour. Res. 27 (5), 783–796.

Williams, G.P., Wolman, M.G., 1984. Downstream effects of dams on alluvial rivers. U.S. Geol. Surv. Prof. Pap. 1286, 64.

Wohl, E., 2012. Identifying and mitigating dam-induced declines in river health: three case studies from the western United States. Int. J. Sediment Res. 27 (3), 271–287. https://doi.org/10.1016/S1001-6279(12)60035-3.

Wohl, E., Bledsoe, B.P., Jacobson, R.B., Poff, N.L., Rathburn, S.L., Walters, D.M., Wilcox, A.C., 2015. The natural sediment regime in rivers: broadening the foundation for ecosystem management. Bioscience 65 (4), 358–371. https://doi.org/10.1093/biosci/biv002.

Wolman, M.G., 1954. A method of sampling coarse river-bed material. Eos, Trans. Am. Geophys. Union 35, 951–956.

Wong, M., Parker, G., 2006. One-dimensional modeling of bed evolution in a gravel bed river subject to a cycled flood hydrograph. J. Geophys. Res.: Earth Surf. 111, F03018. https://doi.org/10.1029/2006JF000478.

Yager, E.M., Dietrich, W.E., Kirchner, J.W., McArdell, B.W., 2012. Prediction of sediment transport in step-pool channels. Water Resour. Res. 48 (1), 1–20. https://doi.org/10.1029/2011WR010829.

Yager, E.M., Kenworthy, M., Monsalve, A., 2015. Taking the river inside: fundamental advances from laboratory experiments in measuring and understanding bedload transport processes. Geomorphology 244, 21–32. https://doi.org/10.1016/j.geomorph.2015.04.002.

Yalin, M.S., 1963. An expression for bed-load transportation. J. Hydraul. Div. Am. Soc. Civ. Eng. 89 (3), 221–250. https://doi.org/10.1061/jyceaj.0000874.

Yarnell, S.M., Petts, G.E., Schmidt, J.C., Whipple, A.A., Beller, E.E., Dahm, C.N., et al., 2015. Functional flows in modified riverscapes: hydrographs, habitats and opportunities. BioScience 65, 963–972. https://doi.org/10.1093/biosci/biv102.

Zhang, C., Xu, M., Hassan, M.A., Chartrand, S.M., Wang, Z., Ma, Z., 2020. Experiment on morphological and hydraulic adjustments of step-pool unit to flow increase. Earth Surf. Process. Landf. 45 (2), 280–294. https://doi.org/10.1002/ESP.4722.